Journal of Sol-Gel Science and Technology (2026)117:39
https://doi.org/10.1007/s10971-025-07045-4

ORIGINAL PAPER

Sol-gel microencapsulated rosemary essential oil as enhanced biopesticide

Giuseppe Angellotti[1] · Antonino Modafferi[2] · Gaetano Giuliano[2] · Mario Pagliaro[1] · Orlando Campolo[2] · Rosaria Ciriminna[1]

Received: 3 October 2025 / Accepted: 21 November 2025

Abstract

Template-driven sol-gel microencapsulation of rosemary (*Rosmarinus officinalis*) essential oil within submicrometric SiO_2 core-shell microcapsules affords a new solid biopesticide dubbed herein "SiliRosm" that can be readily formulated in water, enhancing the stability and bioactivity of the essential oil. Comparing two sol-gel microencapsulation routes to optimize encapsulation efficiency and protection of the bioactive compounds, this study shows that the sol-gel microencapsulation of the essential oil facilitates the sustained release of its molecular components via the Baker–Lonsdale release kinetic model. First results showing high biocidal activity of SiliRosm formulated in water against highly polyphagous *Spodoptera littoralis* are promising toward the practical application of SiliRosm for crop protection.

Graphical abstract

A novel solid biopesticide is prepared by the sol-gel microencapsulation of rosemary essential oil within spherical submicron SiO_2 core-shell microcapsules, which can be effectively formulated in water, showing promising insecticidal activity against polyphagous *Spodoptera littoralis*.

Keywords Silica · *Rosmarinus officinalis* · Sol-gel microencapsulation · Essential oil · *Spodoptera littoralis*

Highlights

- Template-driven sol-gel microencapsulation of *Rosmarinus officinalis* essential oil within submicron-sized spherical silica particles affords a new solid biopesticide.
- Microencapsulation in the core-shell SiO_2 particles enhances the chemical stability and bioactivity of rosemary essential oil.
- Study shows that microencapsulation of the essential oil facilitates the sustained release of its molecular components via the Baker–Lonsdale release kinetic model.

✉ Mario Pagliaro
mario.pagliaro@cnr.it

✉ Orlando Campolo
orlando.campolo@unirc.it

✉ Rosaria Ciriminna
rosaria.ciriminna@cnr.it

[1] Istituto per lo Studio dei Materiali Nanostrutturati, CNR via U. La Malfa 153, Palermo, Italy

[2] Dipartimento di Agraria, Università Mediterranea di Reggio Calabria Loc. Feo di Vito, Reggio Calabria, Italy

Published online: 05 February 2026

- First results showing biocidal activity of SiliRosm formulated in water against highly polyphagous *Spodoptera littoralis* insect are promising toward the practical application of SiliRosm for crop protection.

1 Introduction

Owing to significant antifungal, insecticidal, acaricidal, and antimicrobial properties, coupled with quick biodegradation into non-toxic compounds and lack of detrimental effects on non-target organisms, essential oils (EOs) are widely investigated as biopesticides [1]. Aptly formulated, EOs such as orange oil have been commercialized as ecofriendly pesticide [2]. Noting that the number of commercial biopesticides based on EOs was still low, however, in 2016 Pamela and Benelli concluded that the enhanced use of EO-based biopesticides requires the development of efficient stabilization processes, simplification of the costly biopesticide authorization processes, and optimization of EO extraction processes [3].

Stabilization via microencapsulation is required to provide enhanced chemical and physical protection for the active ingredients against environmental factors such as light, oxygen, and temperature fluctuations, as well as to enable controlled release of the microencapsulated bioactive compounds. Microencapsulation, particularly by in situ polymerization, significantly improves the stability, release behavior, and antimicrobial properties of EOs, enabling large-scale biopesticide development [4]. Commercialization of truly sustainable EO-based biopesticides, however, requires employing cost-effective EOs obtainable in relatively high yield (>1% on a dry weight basis) from plants cultivated on a large scale [5]. Furthermore, to speed up registration, EOs generally recognized as safe (GRAS) or derived from plants with documented use as a food should be preferred [5].

The EO of rosemary (*Rosmarinus officinalis*) is a GRAS substance [6] sourced from a plant ubiquitous in the Mediterranean basin and sub-Himalayan areas, widely employed as a food. The oil is used in folk medicine to alleviate several diseases, including headache, rheumatic pain, nervous agitation, depression, as well as physical and mental fatigue, and is considered for the treatment of people suffering from nervous system disorders [7]. The oil exhibits substantial phytotoxicity [8]. Formulated with natural deep eutectic solvents and microencapsulated via spray drying, the microencapsulated EO shows lower phytotoxicity when employed as a biopesticide [8]. Similarly, microencapsulated in octenyl succinic anhydride – starch matrix particles, the oil substantially increases its persistence, retaining a 46.6% mortality rate against *Tribolium confusum* after 15 days (whereas the non-formulated EO has entirely lost its insecticidal activity) [9].

To the best of our knowledge, the use of as biopesticide of rosemary EO microencapsulated via the sol-gel process has not been reported. Moderate antimicrobial activity of rosemary oil entrapped in methyl-modified silica irregular xerogel microcapsules was reported by Castellón and co-workers in 2016 [10]. Previously, Nasr-Eshafani's team had reported excellent anticorrosion and bonding strength to substrate properties of a similar methylated silica thin film (100 nm thick) doped with 0.05% rosemary EO and further deposited on stainless steel [11].

In this study, we describe the template-driven microencapsulation of rosemary EO within spherical silica microcapsules. Dubbed "SiliRosm" and readily formulated in water, this sol-gel material shows pesticidal activity against *Spodoptera littoralis*. To optimize encapsulation efficiency, water dispersibility, and retention of the bioactive compounds contained in the EO, we compared two SiliRosm sol-gel material preparation routes. Furthermore, to identify the release model, we studied the kinetics of EO release through the mesoporous shell of the silica core-shell microcapsules.

2 Results and discussion

2.1 Encapsulation efficacy

To identify the optimal conditions to achieve high encapsulation efficiency for the hydrophobic EO in core-shell SiO_2 microcapsules, we carried out the sol-gel polycondensation of tetraethylorthosilicate (TEOS) in a microemulsion (using cetyltrimethylammonium bromide as surfactant) [12]. In route "SiliRosm-A", the microparticulate material obtained was filtered and dried in an oven, resulting in a slightly yellow powder (Fig. 1a) whose color may be attributed to the oxidative degradation of certain EO compounds. On the contrary, in route "SiliRosm-B", the material was dispersed in water right after its preparation (Fig. 1b). No particle aggregation or phase separation was observed even months after the preparation of the suspension.

The different dispersibility of SiliRosm microcapsules is due to the evaporation of water during the drying process that leads to the formation of silica microparticle aggregates strongly bound by hydrogen bonds, Van der Waals forces, and capillary forces, resulting in a material that is nearly impossible to redisperse in water [13]. Additionally, the drying process influences the material's capacity to retain essential oils.

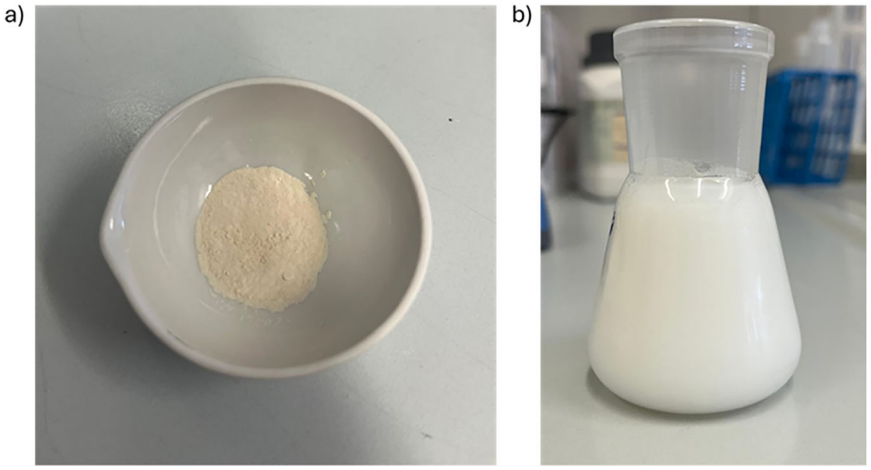

Fig. 1 SiliRosm microcapsules dried (**a**) and dispersed in water without drying (**b**)

Table 1 Chemical composition of commercial rosemary EO and retention time for each compound identified via GC-MS

Compound	Abundance (%)	Retention time (min)
α-pinene	12.6	10.55
Camphene	4.3	11.05
β-pinene	6.8	12.02
d-limonene	2.8	13.84
Eucalyptol	48.9	13.94
γ-terpinene	0.9	14.84
Linalool	0.8	16.21
Camphor	11	17.54
Borneol	3.3	18.20
α-terpineol	2.1	18.97
Bornyl acetate	1.2	21.71
Caryophyllene	5.1	25.26
Others	0.2	

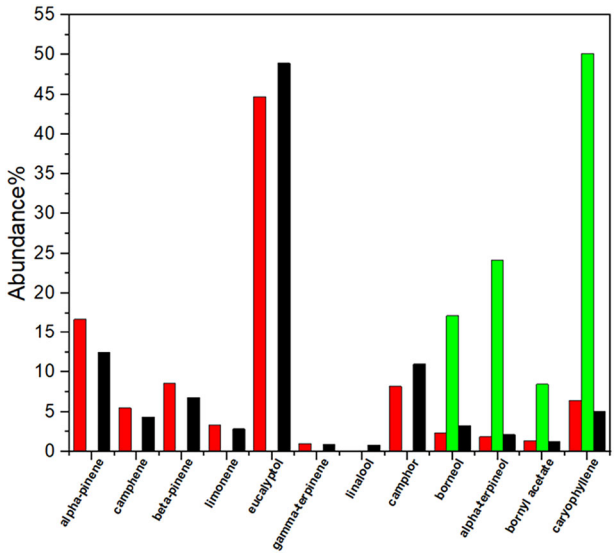

Fig. 2 Abundance (%) of each component of EO in pure essential oil (black), SiliRosm-A (green), and SiliRosm-B (red) microcapsules

Data in Table 1 show that the primary components of the commercial rosemary oil used in this study, identified via gas chromatography-mass spectrometry (GC-MS), are eucalyptol (48.9%), α-pinene (12.6%), camphor (11%), β-pinene (6.8%), and caryophyllene (5.1%). Additionally, the oil contains several other minor constituents in noticeable quantities.

Results in Table 1 highlight that the amount of eucalyptol is very high and larger than that found in other rosemary EOs [14, 15]. Eucalyptol, along with α-pinene, is one of the terpenes responsible for the pesticide activity of the essential oil [16].

The oil contained in SiliRosm-A and SiliRosm-B microcapsules was extracted with ethyl acetate (EtOAc) and analyzed via GC-MS. Data are presented as percentage area for each detected component (Fig. 2).

As expected, the drying process significantly alters the essential oil profile, favoring the preservation of less volatile, higher boiling point terpenes. The composition of the oil extracted from the dried microcapsules comprising SiliRosm-A shows a noticeable reduction in the major terpenes, with only borneol, terpineol, bornyl acetate, and caryophyllene being detected. This result indicates that during the drying process, compounds with lower boiling points, such as α-pinene, camphene, and β-pinene, evaporate alongside water. It is interesting to notice, furthermore, that eucalyptol, regardless of its considerable boiling point (170 °C), is absent in the sample. In contrast, terpenes with a high boiling point (>200 °C) remained entrapped within the microcapsules.

Conversely, the oil extracted from SiliRosm-B microcapsules exhibits a pattern nearly identical to that of the free EO. This shows evidence that the sol-gel microencapsulation process without drying of the resulting microcapsules is highly effective for encapsulating the EO in its entirety.

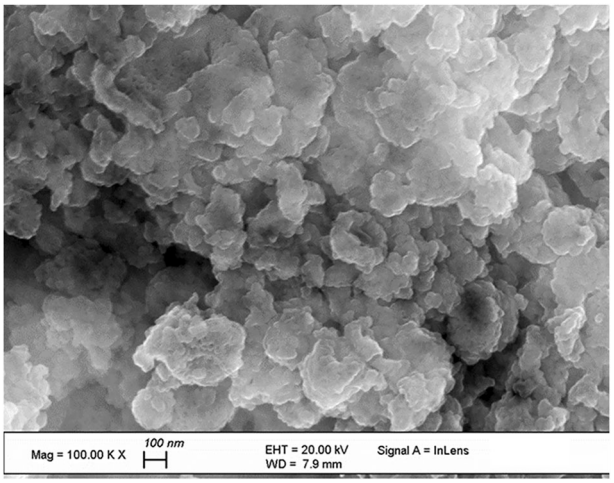

Fig. 3 SEM photograph of SiliRosm (100,000 magnification)

Quantitative analysis supports the previous observations. SiliRosm-A microcapsules exhibit very low oil retention, with an EO encapsulation efficiency of 11.6 ± 0.6% (w/w). The terpene content measured via GC-FID was nearly undetectable, with only caryophyllene being quantified at a concentration <1%. In contrast, the analysis of SiliRosm-B microcapsules revealed a markedly different profile. Both UV-Vis spectrophotometry and GC-FID indeed revealed a high EO encapsulation efficiency of 41 ± 1% (w/w), including 4.8 ± 0.1% α-pinene, 11.6 ± 0.5% eucalyptol, 2.1 ± 0.1% camphor, and 2.1 ± 0.1% caryophyllene.

Disperse systems are susceptible to instability phenomena such as flocculation, particle growth, and sedimentation. Hence, the quantitative analysis of SiliRosm-B material was repeated 3 months after storage at room temperature. Showing evidence of the absence of particle aggregation and precipitation, no significant difference in SiO_2 concentration was detected. Such pronounced stability of the SiliRosm-B microcapsules can be attributed to the relatively large ζ potential (11.2 ± 4.8 mV). Due to the presence of cationic CTAB surfactant molecules at the surface of the silica shell, the relatively large potential contributes to the electrostatic repulsion and colloidal stability of the dispersed microcapsules.

We briefly remind that the relatively high level of variability identified by the SD value of ±4.8 mV is expected and acceptable, especially in the case of submicrometric systems, as opposed to nanometric ones. In colloidal dispersions involving particles in the submicron range, higher heterogeneity in surface area and charge distribution is common, leading to increased variability in zeta potential measurements [17].

Based on these results, we selected the "SiliRosm-B" sol-gel material preparation route as the optimal process for the sol-gel entrapment of rosemary EO in mesoporous SiO_2 microspheres. Consequently, further characterization was performed exclusively on microcapsules, subsequently referred to simply as "SiliRosm", obtained through this route.

2.2 Microcapsule size and morphology

The scanning electron microscopy (SEM) photograph in Fig. 3 shows that SiliRosm consists of silica submicron microcapsules exhibiting a nearly spherical morphology. The irregular surface texture observed in certain microcapsules, such as the presence of fractures, suggests that the capsules possess a porous structure.

The appearance of darker regions in the SEM image may indicate the presence of internal cavities, potentially formed by the evaporation of EO under the high vacuum conditions of the SEM analysis. This phenomenon further confirms the successful encapsulation of the EO within the silica shell. The high concentration of microcapsules in the sample limits the ability to analyze individual particle dimensions via SEM only (diameter of the microcapsules estimated between 150 and 600 nm).

Hence, dynamic light scattering was used to complement the SEM analysis.

The SiliRosm dispersion in water exhibits a hydrodynamic diameter (DH) of 424.7 ± 113.6 nm and a polydispersity index of 0.574, indicating that the sample is relatively homogeneous, with an average particle size in the submicron range.

2.3 Microcapsule textural properties and composition

Evidence of the mesoporous nature of the material suggested by the SEM analysis was obtained by surface textural property analysis relying on adsorption and desorption of cryogenic N_2 at 77.4 K using the Brunauer–Emmett–Teller (BET) equation.

As shown in Fig. 4, the adsorption-desorption isotherms exhibit a strong H2 hysteresis loop characteristic of type IV isotherms with capillary condensation taking place in mesopores [18]. The strong hysteresis loop is due to the presence of large mesopores. This behavior indicates capillary condensation occurring within the pores. Adsorption initiates gradually at low relative pressures, suggesting the presence of micropores, and increases sharply between 0.4 and 0.7 p/p^o, corresponding to the capillary condensation of nitrogen in the mesopores.

The maximum adsorbed volume reaches approximately 400 cm^3/g (STP), indicating a specific surface area of 279.5 m^2/g. The porosity analysis, conducted using the BJH method, reveals a predominant pore diameter of 5.02 nm, with a pore specific volume of 0.67 cm^3/g.

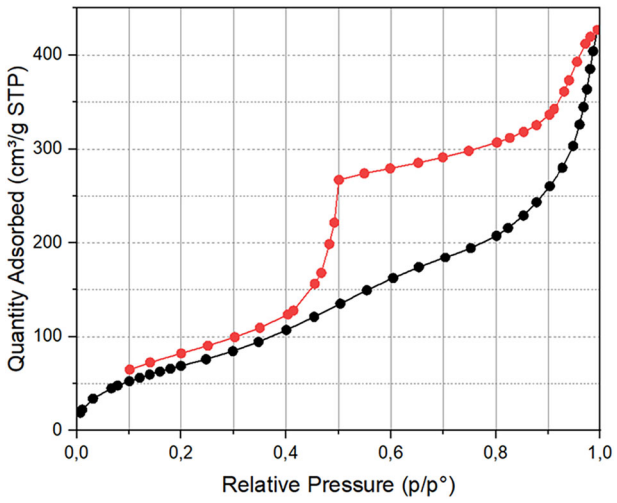

Fig. 4 Adsorption-desorption isotherms of cryogenic N_2 for SiliRosm

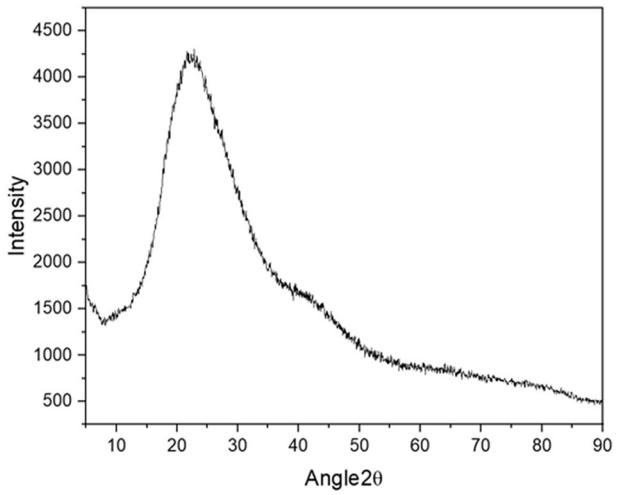

Fig. 5 XRD pattern of SiliRosm

The XRD pattern (Fig. 5) shows evidence that SiliRosm consists of an amorphous silica structure with its characteristic broad peak centered around 22°, characteristic of the short-range ordering (periodicity) within the tetrahedral (SiO_4) basic unit in which the latter units are joined in a random manner with no periodicity in their arrangements [19].

SiliRosm, rosemary oil, and empty microcapsules were further analyzed via attenuated total reflection Fourier transform infrared (ATR-FTIR) spectroscopy. The spectrum of the EO (Fig. 6, black spectrum) is chiefly characterized by absorption bands corresponding to eucalyptol.

A strong signal at 985 cm^{-1} is attributed to the symmetrical bending of the methylene groups. Additional peaks observed at 1079 cm^{-1} and 1214 cm^{-1} are assigned to the symmetric and asymmetric stretching of the C–O–C group, respectively. Furthermore, the peak at 1375 cm^{-1} represents the deformation band of the $–CH_3$ group. Notably, a peak at

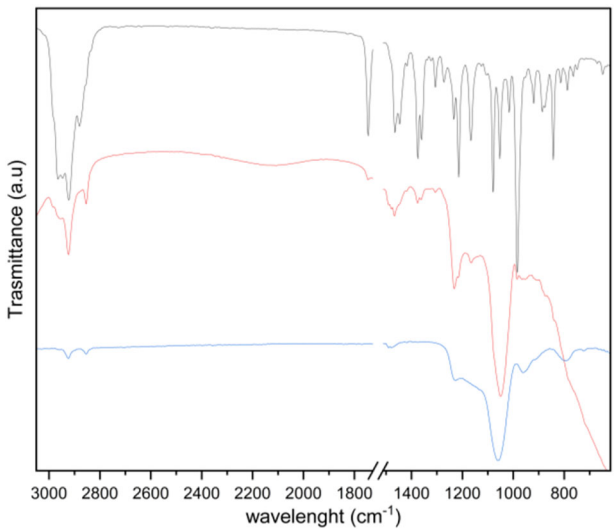

Fig. 6 FTIR spectra of pure EO (black line), SiliRosm (red line), and empty SiO_2 microcapsules (blue line)

1747 cm^{-1} corresponds to the stretching of the –C=O group, which is associated with camphor. Peaks in the wavenumber range 2800–3000 cm^{-1} are characteristic of C–H alkyl groups stretching.

In contrast, the spectrum of the empty microcapsules exhibits (Fig. 6, blue line) the characteristic peaks of SiO_2, including a pronounced band at 1100 cm^{-1} and a peak at 810 cm^{-1}, corresponding to the asymmetric and symmetric stretching vibrations of Si–O–Si bonds.

Finally, the spectrum of SiliRosm (Fig. 6, red line) appears as a superimposition of the spectra of the EO and the empty microcapsules.

Notably, the band at 1100 cm^{-1} remains prominent, coexisting with the principal peaks attributed to the essential oil. The absence of any shift in absorption peaks confirms that the essential oil is physically encapsulated within the microcapsules without chemical modification of the sol-gel entrapped molecules.

2.4 Microcapsule release behavior

To evaluate the ability of SiliRosm to retain and control the release of essential oil, a release investigation was conducted. Designing the experimental setup was challenging due to the inherent difficulty in replicating real-world application conditions in a laboratory setting. Numerous environmental variables, indeed, such as daily and seasonal fluctuations in humidity, light, and temperature, significantly influence open-field conditions. Additionally, the release mechanism relies on the evaporation of the EO from within the microcapsules.

Assessing this process in the form of a water dispersion presents methodological complexities. For this reason, the experiment was intentionally designed under accelerated

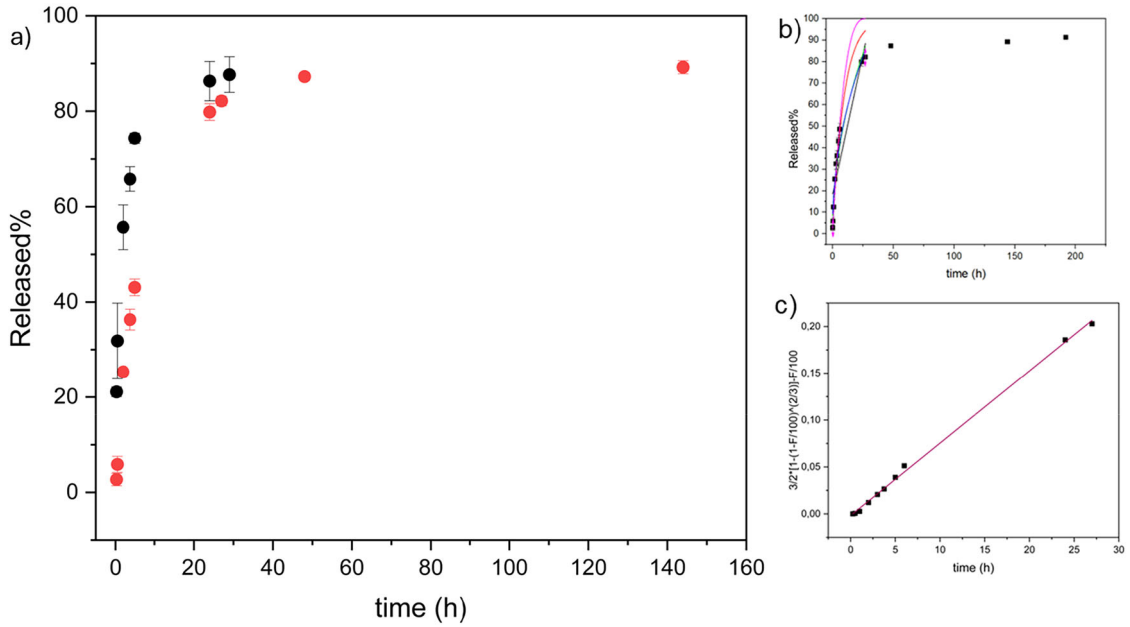

Fig. 7 **a** Release patterns of EO as percentage of EO released over time from solution (black line) and SiliRosm (red); **b** kinetic model fitting at 27 h: Zero Order (black), First Order (red), Higuchi (green), Korsmeyer–Peppas (blue), Hixon–Crowell (purple). **c** Backer–Lonsdale kinetic fitting

Table 2 Kinetic models and corresponding parameters and correlation coefficients derived from fitting the rosemary EO release from SiliRosm

Mathematical models	Equations	Parameters	R^2
Zero order	$F = k_0 t$	$k_0 = 3.543$	0.563
First order	$F = 100*[1 - \mathrm{Exp}(-k_1 t)]$	$k_1 = 0.102$	0.943
Higuchi	$F = k_H t^{0.5}$	$k_H = 16.737$	0.966
Korsmeyer–Peppas	$F = k_{KP} t^n$	$k_{KP} = 18.130$ $n = 0.47$	0.959
Hixon–Crowell	$F = 100[1 - (1 - k_{HC} t)^3]$	$k_{HC} = 0.027$	0.866
Baker–Lonsdale	$3/2[1 - (1 - F/100)^{2/3}] - F/100 = k_{BL} t$	$k_{BL} = 0.0077$	0.998

conditions to reach at least 80% of the total release, allowing us to characterize the release kinetics and apply mathematical modeling. It is important to note that in this type of study, essential oil solubility must not act as the limiting factor; otherwise, the retention capability of the capsules could not be properly evaluated. Therefore, we designed a study to evaluate the technological performance of SiliRosm in controlling the release of essential oil, comparing the results with those obtained from a reference experiment performed in the same conditions using the EO in solution.

A dialysis membrane was chosen with a cut-off below the diameter of the microcapsules in order to study only the diffusion of the essential oil from the donor to the acceptor chamber. The EO release pattern over time in Fig. 7a shows that the diffusion rate of EO in solution was significantly faster than that of EO released from microcapsules, with 22% released from the solution compared to a mere 2.4% from the SiliRosm core-shell microcapsules.

This trend persisted for the whole experiment, although a deceleration in the release rate was noted after 30 h, due to a reduction in the concentration gradient. The difference in the release pattern between free and sol-gel micro-encapsulated EO is indicative of enhanced retention efficacy of EO components within the silica shell of the SiliRosm mesoporous microcapsules, which plays a crucial role in sustaining the controlled and prolonged release of the EO. Several kinetic release models were thus applied to the experimental data to identify the release mechanism.

Analyzing the correlation coefficient (R^2) of each mathematical model applied to the experimental data revealed that the two kinetic equations that best describe the release mechanism of rosemary EO from the SiliRosm spherical microcapsules are the Higuchi and Baker–Lonsdale models (Table 2). Indeed, Higuchi originally formulated his release kinetic model to describe the release of poorly soluble drugs from an inert matrix system remaining unaffected by erosion or swelling phenomena [20].

However, the Higuchi model does not account for the geometry of the system. In 1974, Baker and Lonsdale refined Higuchi's kinetics, adapting it specifically to spherical matrix systems [21]. Details on the other kinetic models employed can be found in a comprehensive account [22].

The plots of each kinetic equation alongside the experimental data are shown in Fig. 7b. The Baker–Lonsdale straight line (Fig. 7c) corresponds to a linear equation.

Both models, particularly the Baker–Lonsdale model, are representative of the release mechanism from SiliRosm microcapsules. Indeed, in agreement with the well-known lack of swelling of inherently rigid silica microparticles in water [12], the mesoporous shell of SiO_2 comprising the SiliRosm microcapsules does not exhibit significant swelling or dissolution phenomena, behaving as a monolithic material that fits perfectly into the framework described by the Baker–Lonsdale model.

Further evidence supporting the Higuchi-type release kinetics originates from the application of the Korsmeyer–Peppas model, where the exponent n provides insights into the type of kinetics being observed. In our case, the n value is 0.47, characteristic of Higuchi kinetics in which n amounts to 0.5.

These findings are highly significant, as they confirm that, from a technological perspective, the SiliRosm microcapsules effectively retain the rosemary EO and release it in a controlled manner over time by Fickian diffusion with no microparticle degradation or erosion occurring, following a well-defined (Baker–Lonsdale) kinetic equation.

Finally, the pesticide activity of SiliRosm was evaluated using *Spodoptera littoralis* as the pest model. A highly polyphagous insect, *S. littoralis* is one of the most destructive agricultural lepidopterous pests within its subtropical and tropical range [23]. Economically relevant crops and plants attacked by this species include tomato, cotton, ornamental flowers, apple, grape, and clover. Numerous synthetic insecticides are used to control this pest, whose reported resistance to many insecticidal compounds increases the potential for damage [24].

The black histograms in Fig. 8 show that no change in pest viability was observed using control sample materials, including water with surfactant CTAB, and empty SiO_2 microcapsules. On the other hand, the application of the rosemary EO emulsion resulted in a time-dependent reduction in pest viability, with a maximum reduction to 70% viability observed after 72 h of treatment. Notably, when the SiliRosm formulation was administered, pest viability decreased significantly, reaching approximately 50% after 72 h. Despite the high content of EO encapsulated within the microcapsules, no structural damage to zucchini leaves was observed, showing preliminary evidence of lack of phytotoxicity.

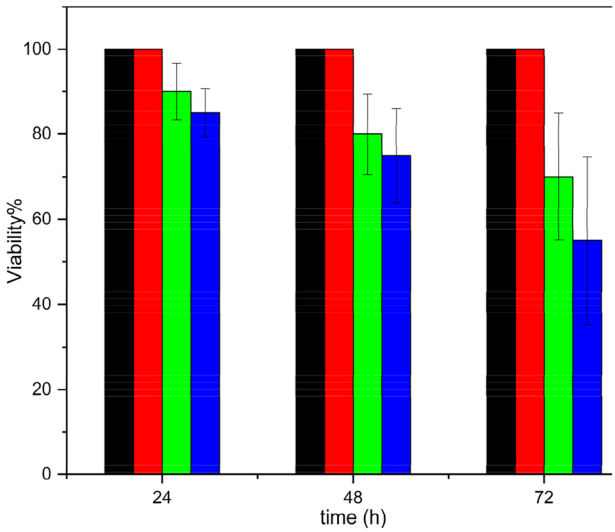

Fig. 8 *Spodoptera littoralis* viability after 72 h treatment with water plus surfactant (black bar), empty microcapsules (red), EO microemulsion (green), and SiliRosm (blue)

Even though lacking randomization and blinding, as well as requiring larger sample sizes and dose–response analysis, the bioassay preliminary results are promising and serve as proof of concept for the efficacy of the SiliRosm microencapsulated biopesticide on the highly polyphagous *Spodoptera littoralis* insect. We briefly remind that EOs exert their insecticidal activity through a combination of contact and ingestion modes of absorption, with the latter ingestion occurring both orally and through the tracheal system, and the toxic contact activity mainly caused by toxic compounds in the EO penetrating through the cuticle. Said mechanisms explain why EOs are generally not employed as insecticides due to their high volatility and low persistence [25].

Likewise to what was found with the release of EO from spherical sol-gel microparticles encapsulating orange essential oil [26], we ascribe the enhanced efficacy of EO released by the SiliRosm microcapsules to the large surface area of the inner mesoporosity of the core-shell microcapsules that promotes contact of the entrapped EO with the insect. On the other hand, the microencapsulation of the EO within the SiO_2 core-shell microcapsules protects the entrapped volatile bioactives and prevents their quick evaporation [27]. Indeed, prior to pest exposure, the bioactive formulations were allowed to dry, which facilitates essential oil evaporation. Said evaporation was more pronounced in the EO emulsion, whereas the microencapsulation of the EO in the core of the core-shell SiliRosm microcapsules limited the EO evaporation and controlled its release.

In summary, we have discovered that the sol-gel microencapsulation of *Rosmarinus officinalis* essential oil within spherical mesoporous SiO_2 microcapsules of submicrometric size, subsequently formulated as a water-based dispersion, affords an effective biopesticide against the highly polyphagous *Spodoptera littoralis* insect.

The high (41 wt%) essential oil encapsulation efficiency within the mesoporous SiO_2 shell promotes the microcapsule capacity to retain and gradually release the single components of the essential oil. The sol-gel encapsulation ensures effective entrapment of key terpenes like eucalyptol and α-pinene, crucial for pesticidal and acaricidal activity [28]. The mesoporous silica structure further facilitates sustained release that takes place in agreement with the Baker–Lonsdale model of release of poorly soluble drugs from an inert spherical matrix, remaining unaffected by erosion or swelling phenomena. The inertness of the silica matrix, furthermore, enables controlled diffusion without swelling or dissolution phenomena.

Highlighting the stability of SiliRosm biopesticide, no significant changes in stability and encapsulation efficiency were detected after three months of storage at room temperature. Preliminary findings, furthermore, indicate a lack of SiliRosm phytotoxicity (no changes in the zucchini plant leaf treated), whereas the pure oil exerts substantial phytotoxicity. The submicron 0.42 µm size of the functionalized SiO_2 microcapsules comprising SiliRosm is ideally suited for application on plants, while their dispersion in water only intrinsically prevents health and safety risks for farmers and operators. Remarkably, indeed, recent findings indicate that supplementation of SiO_2 nanoparticles having 200 m^2/g surface area to *Mentha arvensis* (menthol mint) plants stressed by Cu exhibits beneficial antioxidant effects on the Cu-disturbed plants, lowering reactive oxygen species production and improving EO production [29].

From a practical viewpoint, stabilization and bioactivity enhancement of rosemary EO through sol-gel entrapment within mesoporous SiO_2 core-shell microcapsules not only extends the shelf life of the EO but would also reduce the frequency of applications, thereby minimizing the economic cost of real application in crop protection.

It is also relevant, in view of practical applications, that rosemary EO (REO, manufactured via hydrodistillation in many of said countries) is sourced in high yield (>1% on a dry weight basis [5]) from a wild plant ubiquitous in Mediterranean basin countries, where it is cultivated on a large scale. As a result, the EO has a relatively low price. For example, highly pure EO for pharmaceutical applications was sold online by mid-2025 at about $17/kg [30]. A significantly lower price will be applied when purchasing the oil in large batches.

The environmental fate and safety assessment of SiliRosm and other mesoporous submicrometric SiO_2 particles encapsulating EOs will be the outcomes of a subsequent investigation. It is encouraging to learn that research on cytotoxicity of spherical mesoporous SiO_2 particles with particle sizes of 190, 420, and 1220 nm found that cytotoxicity is highly correlated with particle sizes, with particles of 1220 nm showing slight cytotoxicity and 420 nm microparticles showing significant cytotoxicity only at concentrations above 25 mg/mL [31].

Future work will investigate how the insects start the process of interaction with the product (SiliRosm) conducting several trials at different doses and define a population parameter, such as the median lethal dose (LD_{50}) which kills 50% of the population, typically used as indicator of acute toxicity, including comparative assessment of the 95% confidence limits (LCs) of a lethal dose ratio to indicate whether the lethal doses of the two toxicants are statistically different from one another [32].

3 Conclusions

In conclusion, the sol-gel entrapment of abundant and economically viable rosemary essential oil in spherical SiO_2 microcapsules reported in this study is promising toward the development of an environmentally friendly and economically viable alternative to synthetic pesticides for sustainable pest management for one of the most crop-destructive insects (*Spodoptera littoralis*). The biopesticide, indeed, can be effectively dispersed (formulated) in water.

Future studies will investigate the effectiveness and ecological safety of SiliRosm biopesticide formulated in water under real-world conditions.

4 Experimental section

4.1 Materials

Rosmarinus officinalis essential oil (product number W299200, Merck), tetraethylorthosilicate (TEOS, ≥99.0% purity), cetyltrimethylammonium bromide (CTAB, molecular biology grade), 25% ammonia solution (for HPLC), glycerol (≥99.0%), α-pinene (≥99%), eucalyptol (≥99%), camphor (1 *R* enantiomer, 98%), caryophyllene, (≥98.0%, sum of enantiomers), and undecane (≥99%) were purchased by Merck KGaA (Darmstadt, Germany). All solvents used were of analytical grade.

4.2 Sol-gel microencapsulation of *Rosmarinus officinalis* EO

The REO-doped microcapsules were prepared using the sol-gel method with an O/W microemulsion as the template.

First, a solution containing 12.5 mL of REO and 14.52 mL of TEOS was prepared. This solution was then mixed with 250 mL of a previously prepared aqueous phase consisting of distilled water supplemented with 10% v/v glycerol and 2% w/v CTAB. The microemulsion was obtained by combining the two phases using an Ultraturrax for 1 min, followed by 10 min of treatment with a probe high-frequency sonicator set to 30% amplitude in pulse mode, while maintaining the sample in an ice/water bath. After preparation, an aliquot of the resulting microemulsion was collected and analyzed using a Malvern Zetasizer to determine the hydrodynamic diameter of the droplets. Subsequently, the microemulsion was transferred into a round-bottom flask, and 2.5 mL of a 25% ammonium hydroxide solution was added. The mixture was stirred at 40 °C for 72 h, resulting in a white dispersion. The sample was then divided into two equal batches. The first batch was dried in an oven at 35 °C for 3 h and labeled as SiliRosm-A. The second batch was dispersed in 100 mL of distilled water and stored at 4 °C for further use, labeled as SiliRosm-B. These two preparation strategies were compared to determine the optimal method. As described, empty microcapsules were prepared and managed using n-hexane as the internal phase.

4.3 Essential oil and microcapsule composition

The composition of both the pure rosemary essential oil and the EO encapsulated within the microcapsules was tentatively characterized via gas chromatography-mass spectrometry (GC-MS). The selected chromatographic parameters for each analysis were kept across all experimental runs. An Agilent 6890 chromatograph (Agilent Technologies, Santa Clara, CA, USA) coupled to a mass-selective detector Agilent 5975, was utilized for the analyses. The stationary phase was a 5% methylsiloxane capillary column (Agilent Technologies, 30 m length, 0.25 mm internal diameter, 0.25 µm film thickness). The injector was kept at 250 °C and operated in split mode with a split ratio of 2:1. The chromatographic conditions included a He carrier gas flow rate of 1 mL/min and an oven temperature program initiated with a 5 min isothermal hold at 40 °C, followed by a linear temperature ramp of 5 °C/min up to 200 °C followed by a gradient of 10 °C/min to 250 °C. The entire run lasted 50 min. The mass spectrometry settings were as follows: ion source temperature 250 °C, interface temperature 280 °C, electron ionization energy at 70 eV, and mass scan range of 50–550 amu. Molecular identification was performed using the Wiley Registry/NIST Mass Spectral Library 2023.

In brief, aliquots of SiliRosm were filtered, and the hydrated solid residue was extracted with 5 mL of ethyl acetate to isolate the encapsulated EO. The resulting solutions were dehydrated using anhydrous sodium sulfate prior to analysis. For comparison, a standard solution of pure REO was prepared in ethyl acetate.

For quantitative analysis, 10 mg of SiliRosm-A sample was dispersed in 2 mL of EtOAc and the EO extracted for 1 h under magnetic stirring. The resulting coarse dispersion was filtered through a 0.22 µm filter, dehydrated with anhydrous Na_2SO_4, and analyzed by GC-FID and UV-Vis spectroscopy as described below. To evaluate the encapsulation efficiency of SiliRosm-B, a different strategy was employed. First, the concentration of microcapsules per unit volume of the dispersion was determined. A 5 mL sample of the dispersion was filtered and dried in an oven. The weight of the residual dry material was used to calculate the microcapsule concentration. Subsequently, a 1 mL aliquot of the SiliRosm dispersion was withdrawn, shaken to ensure homogeneity, and filtered using a Whatman glass fiber filter. The liquid filtrate was collected and treated with EtOAc to extract any dissolved components. The solid residue was then thoroughly dispersed in 10 mL of EtOAc and kept under stirring for 1 h. This mixture was filtered and analyzed by GC-FID and UV-Vis spectroscopy. The ethyl acetate extract of the liquid filtrate was processed similarly.

The results from UV-Vis analysis are reported as the percentage of the total EO encapsulated, while the GC-FID results were used to determine the percentage of the major terpenes within the SiliRosm microcapsules. The amounts were calculated using the following equations:

$$\mathrm{EO}(\%) = [\mathrm{Q\_EO}/(\mathrm{Q\_Solid} + \mathrm{Q\_(EO)}] \times 100 \quad (1)$$

$$\mathrm{Terpene}(\%) = [\mathrm{Q\_terpene}/(\mathrm{Q\_Solid} + \mathrm{Q\_EO})] \times 100 \quad (2)$$

where Q_EO and Q_terpene are the amounts of essential oil and selected terpene (pinene, eucalyptol, camphor and caryophyllene) as determined by UV-Vis and GC-FID, respectively, and Q_Solid is the mass of the dry silica microcapsules. The quantitative analysis was used as a critical parameter to select the optimal microcapsule preparation strategy. Subsequent characterizations were performed on SiliRosm-B, in the following referred to as "SiliRosm". Quantitative analysis was repeated after 3 months of static storage of SiliRosm to assess its stability over time.

UV-Vis spectrophotometric analysis was carried out using a Shimadzu UV-1800 (Shimadzu, Kyoto, Japan). For quantitative analysis, an EO calibration curve in EtOAc was obtained by preparing five different solutions and analyzing them along with a blank. The signals were recorded at $\lambda_{max} = 266$ nm. The calibration curve was obtained by plotting the absorbance values against the respective solution concentration. A blank analysis conducted using EtOAc-based extract of empty microcapsules revealed no

detectable peaks, confirming the absence of interference with other components.

The parameters of the EO calibration curve and the linear fit equation were as follows:

range concentration, 0.1–1.78 mg/mL

$$y = -0.0064 + 0.5986 \times [\text{mg/mL}, (R^2 = 0.999)] \quad (3)$$

To quantify the amount of EO in the release study, a calibration curve in water:isopropanol solution was prepared, considering the $\lambda_{max} = 266$ nm.

The parameters and the linear fit equation were as follows:

range concentration, 0.005–0.5 mg/mL

$$y = 0.048 + 0.6343 \times [\text{mg/mL}, (R^2 = 0.999)] \quad (4)$$

The GC-FID analysis was performed to quantify the amount of each terpene microencapsulated. Assessment was carried out using a Shimadzu GC-FID 17 A gas chromatograph with a 50–250 °C temperature range using a ramp rate of 10 °C/min. The GC was equipped with a flame ionization detector (FID) for compound detection. The chromatographic separation utilized a Supelco SPB-1701 capillary column (Supelco, Bellefonte, PA, USA). For the quantitative determination of the target compounds, calibration curves were constructed. Standard solutions with known concentrations in ethyl acetate were prepared.

These solutions, containing the internal standard undecane, were injected into the GC-FID using an injection syringe. Calibration curves were obtained by plotting the ratio between the signal of each terpene and undecane against the corresponding analyte concentrations. The parameters for each analyte and the respective calibration linear fit equations were as follows:

a-pinene: range concentration, 0.031–0.49 mg/mL; retention time: 6.2 min;

$$y = -0.0014 + 9.0259 \times [\text{signal} - \text{ratio pinene/undecane};(R^2 = 0.999)] \quad (5)$$

Eucalyptol: range concentration 0.069–0.555 mg/mL; retention time: 7.8 min

$$y = 0.0242 + 9.4349 \times [\text{signal} - \text{ratio eucalyptol/undecane};(R^2 = 0.999)] \quad (6)$$

Camphor: range concentration, 0.01 - 0.20 mg/mL; retention time: 12 min

$$y = -0.0225 + 11.098 \times [\text{signal} - \text{ratio camphor/undecane};(R^2 = 0.999)] \quad (7)$$

Caryophyllene: range concentration, 0.031–0.50 mg/mL; retention time: 15.10 min

$$y = -0.0334 + 8.7878 \times [\text{signal} - \text{ratio caryophyllene/undecane};(R^2 = 0.999)] \quad (8)$$

4.4 SEM, ζ-potential, BET, XRD, and FTIR analyses

The morphology of the microcapsules was analyzed by Scanning Electron Microscopy (SEM) using a Zeiss LEO 1530 (Carl Zeiss NTS, Oberkochen, Germany) high-resolution electronic field emission scanning microscope (FE-SEM) with an accelerating voltage of 20 kV. The size distribution and ζ-potential of SiliRosm microcapsules dispersed in water diluted 10-fold with distilled water were obtained by a Malvern Zetasizer Nano ZS (Malvern Panalytical, Malvern, Great Britain). Results are the means of three measurements.

The specific surface area (SSA), pore specific volume (PSV), and pore size distribution of the microcapsules were obtained by measuring the N_2 adsorption-desorption isotherms, performed with a NOVA 2000e surface area and pore size analyzer (Quantachrome, Boynton Beach, FL, USA). Nitrogen at 77 K served as the adsorbate. To assess the structural properties of SiliRosm, aliquots of the dispersion in water were filtered through a 0.45 µm Whatman filter and subsequently dried in an oven at 60 °C for 3 h prior to the BET analysis and XRD measurements.

Samples were degassed under vacuum at approximately 30 °C overnight before analysis. The SSA was calculated using the multipoint Brunauer–Emmett–Teller (BET) method, based on adsorption and desorption data within a relative pressure (p/p_o) range of 0–0.98 at 77.4 K. Pore size distribution and specific pore volume were determined using the Barrett-Joyner-Halenda (BJH) model, applied to the desorption branch of the isotherms across the full p/p_o range.

The X-ray diffraction (XRD) measurements were performed using a D5005 X-ray diffractometer (Bruker AXS, Karlsruhe, Germany) operating at 40 kV and 30 mA. Diffraction patterns were acquired at a scan rate of 0.15°/min over the 10°–80° scattering angle (2θ) range. The X-ray radiation, generated from a copper (Kα) anode, was monochromatized using the instrument's secondary monochromator.

The Fourier Transform Infrared (FTIR) analysis was conducted using a Bruker (Billerica, MA, USA) FTIR instrument in attenuated total reflection (ATR) mode, equipped with a Transit Platinum ATR probe and a diamond crystal. For the analysis of both SiliRosm and empty microcapsules, the dispersion was in each case filtered to remove excess water before immediate analysis. Measurements were conducted within the 600–4000 cm^{-1} wavenumber range, with a spectral resolution of 2 cm^{-1}.

Each spectrum was acquired by averaging 128 scans to enhance the signal-to-noise ratio. A background spectrum was recorded under identical conditions and automatically subtracted from the sample spectra to minimize atmospheric interference.

4.5 Release behavior

The study of EO release from SiliRosm microcapsules was conducted using a dialysis tube method. In summary, the SiliRosm sample was diluted in a water:isopropanol 1:1 solution. A 1 mL portion was placed into a dialysis tube (12.5 kDa, Millipore). The tube was then dipped into 10 mL of the same H_2O:*i*-PrOH solution kept under magnetic stirring at room temperature. At specific time intervals, 1 mL samples were taken from the acceptor compartment, quickly replaced with the fresh solvent to maintain the sink condition, and analyzed using UV-Vis spectrophotometry using a Shimadzu UV-1800 (Kyoto, Japan).

A solution of pure EO in *i*-PrOH was analyzed using the same spectrometer. The results were expressed as the cumulative percentage of EO released over time. Data obtained were fitted to several mathematical models that describe release mechanisms from various delivery systems, including Zero Order, First Order, Higuchi, Hixson–Crowell, Hopfenberg, Baker–Lonsdale, and Korsmeyer–Peppas. Data analysis was performed using Origin Pro 8.5 (Origin Lab, Northampton, MA, USA) and Microsoft Excel (Microsoft Corporation, Redmond, WA, USA) with the DD Solver extension (CIT). The best fit was determined by considering the correlation R^2 values along with the best visual alignment with the experimental curves.

4.6 Pesticidal activity assessment

To evaluate the insecticidal properties of SiliRosm, a dip-test analysis was conducted using zucchini leaf samples. Leaf disks (approximately 2 cm in diameter) were carefully cut and submerged in one of the following treatments: SiliRosm (500 mg dispersed in 150 mL of ultrapure water), empty microcapsules (500 mg dispersed in 150 mL of ultrapure water), an O/W rosemary EO microemulsion prepared adding to a water solution supplemented with surfactant the 5% (w/v) of EO (control) according to the methodology already described above for the preparation of SiliRosm.

After dipping, each sample was allowed to air dry at room temperature to remove excess liquid. The treated leaf disks were then placed individually into Petri dishes. Each treatment group was exposed to five third-instar larvae of *Spodoptera littoralis*. The Petri dishes were sealed to prevent essential oil evaporation and to maintain consistent exposure conditions [33]. The pest behavior, feeding activity, and larval viability were monitored and assessed after 72 h of treatment. Observations included larval mortality, leaf damage, and any visible signs of deterrence or toxic effects.

4.7 Statistical analysis

All experiments were performed at least in triplicate. Data are expressed as mean values ± standard deviation (SD). The experimental data, graph, and statistical analysis were processed using OriginPro (OriginLab, Northampton, MA, USA) as software. Differences between groups were evaluated using Student's *t*-test, with a p-value < 0.05 considered statistically significant. Given the low variability observed among replicates, the number of replicate experiments was deemed adequate for this preliminary study

Data availability

Data supporting the findings of this study are available from the corresponding authors upon reasonable request.

Acknowledgements We thank Dr Gabriella Di Carlo and Dr Francesco Giordano, Istituto per lo Studio dei Materiali Nanostrutturati, CNR, for the SEM and XRD measurements.

Author contributions G.A. prepared the materials. A.M. and G.G. conducted the experiments on the insects. M.P. wrote the main manuscript text. O.C. and R.C. revised the draft text. R.C., O.C., and M.P. conceived the study and supervised the research. All authors reviewed the manuscript.

Funding Funding was received from Ministero dell'Università e della Ricerca, Progetto "FutuRaw. Le materie prime del futuro da fonti non-critiche, residuali e rinnovabili", Fondo Ordinario Enti di Ricerca, 2022 (CUP B53C23008390005). Work of GA was supported by SAMOTHRACE (Sicilian Micro and Nano Technology Research and Innovation Center) Innovation Ecosystem - European Union NextGeneration EU (PNRR – Mission 4 Component 2, Investment 1.5, ECS00000022).

Compliance with ethical standards

Conflict of interest The authors declare no competing interests.

Publisher's note Springer Nature remains neutral with regard to jurisdictional claims in published maps and institutional affiliations.

References

1. Assadpour E, Can Karaça A, Fasamanesh M et al. (2023) Application of essential oils as natural biopesticides; recent advances. Crit Rev Food Sci Nutr 64:6477–6497. https://doi.org/10.1080/10408398.2023.2170317
2. Ciriminna R, Meneguzzo F, Pagliaro M (2017) Orange oil. In: Nollet LML, Singh Rathore H (eds) Green Pesticides Handbook: Essential Oils for Pest Control. Routledge, pp 291–302. https://doi.org/10.1201/9781315153131-15
3. Pavela R, Benelli G (2016) Essential oils as ecofriendly biopesticides? Challenges and constraints. Tr Plant Sci 21:1000–1007. https://doi.org/10.1016/j.tplants.2016.10.005
4. Fakhariha M, Rafati AA, Garmakhany AD, Zolfaghari Asl A (2025) Nanoencapsulation enhances stability, release behavior, and antimicrobial properties of sage and thyme essential oils. Sci Rep 15:18373. https://doi.org/10.1038/s41598-025-00022-5
5. Giunti G, Benelli G, Palmeri V et al. (2022) Non-target effects of essential oil-based biopesticides for crop protection: Impact on natural enemies, pollinators, and soil invertebrates. Biol Control 176:105071. https://doi.org/10.1016/j.biocontrol.2022.105071
6. Aguilar F, Autrup H, Barlow S et al. (2008) Use of rosemary extracts as a food additive - scientific opinion of the panel on food additives, flavourings, processing aids and materials in contact with food. EFSA J 721:1–29. https://doi.org/10.2903/j.efsa.2008.721
7. Rahbardar MG, Hosseinzadeh H (2020) Therapeutic effects of rosemary (*Rosmarinus officinalis* L.) and its active constituents on nervous system disorders. Iran J Basic Med Sci 23:1100–1112. https://doi.org/10.22038/ijbms.2020.45269.10541
8. Dunan L, Malanga T, Benhamou S et al. (2023) Effects of essential oil-based formulation on biopesticide activity. Ind Crop Prod 202:117006. https://doi.org/10.1016/j.indcrop.2023.117006
9. Ahsaei SM, Rodríguez-Rojo S, Salgado M et al. (2020) Insecticidal activity of spray dried microencapsulated essential oils of *Rosmarinus officinalis* and *Zataria multiflora* against *Tribolium confusum*. Crop Prot 128:104996. https://doi.org/10.1016/j.cropro.2019.104996
10. Vega O, Araya JJ, Chavarría M et al. (2016) Antibacterial biocomposite materials based on essential oils embedded in sol–gel hybrid silica matrices. J Sol-Gel Sci Technol 79:584–595. https://doi.org/10.1007/s10971-016-4045-9
11. Motalebi A, Nasr-Esfahani M (2013) Electrochemical and in vitro behavior of nanostructure sol-gel coated 316L stainless steel incorporated with rosemary extract. J Mater Eng Perform 22:1756–1764. https://doi.org/10.1007/s11665-012-0448-0
12. Pagliaro M, Sciortino M, Ciriminna R et al. (2011) From molecules to systems: sol-gel microencapsulation in silica-based materials. Chem Rev 111:765–789. https://doi.org/10.1021/cr100161x
13. Rahman IA, Vejayakumaran P, Sipaut CS et al. (2008) Effect of the drying techniques on the morphology of silica nanoparticles synthesized via sol–gel process. Ceram Int 34:2059–2066. https://doi.org/10.1016/j.ceramint.2007.08.014
14. Jiang Y, Wu N, Fu YJ et al. (2011) Chemical composition and antimicrobial activity of the essential oil of rosemary. Environ Toxicol Pharmacol 32:63–68. https://doi.org/10.1016/j.etap.2011.03.011
15. Hussain AI, Anwar F, Chatha SA et al. (2019) *Rosmarinus officinalis* essential oil: antiproliferative, antioxidant and antibacterial activities. Braz J Microbiol 41:1070–1078. https://doi.org/10.1590/S1517-838220100004000027
16. Obeng-Ofori D, Reichmuth C, Bekele J (2009) Biological activity of 1,8 cineole, a major component of essential oil of *Ocimum kenyense* (Ayobangira) against stored product beetles. J Appl Entomol 121:237–243. https://doi.org/10.1111/j.1439-0418.1997.tb01399.x
17. Angellotti G, Riccucci C, Di Carlo G et al. (2024) Towards sustainable pest management of broad scope: sol-gel microencapsulation of *Origanum vulgare* essential oil. J Sol-Gel Sci Technol 112:230–239. https://doi.org/10.1007/s10971-024-06512-8
18. Sing KSW, Everett DH, Haul RAW et al. (1985) Reporting physisorption data for gas/solid systems with special reference to the determination of surface area and porosity. Pure Appl Chem 57:603–619. https://doi.org/10.1351/pac198557040603
19. Biswas RK, Khan P, Mukherjee S et al. (2018) Study of short range structure of amorphous Silica from PDF using Ag radiation in laboratory XRD system, RAMAN and NEXAFS. J Non-Cryst Solids 488:1–9. https://doi.org/10.1016/j.jnoncrysol.2018.02.037
20. Higuchi T (1961) Rate of release of medicaments from ointments bases containing drugs in suspension. J Pharm Sci 50:874–875. https://doi.org/10.1002/jps.2600501018
21. Baker RW, Lonsdale HS (1974) Controlled release: mechanisms and rates. In: Tanquary AC, Lacey RE (eds) Controlled Release of Biologically Active Agents. Plenum Press, New York, NY, USA; pp 15–72.
22. Bruschi ML (2015) Mathematical models of drug release. In: Bruschi ML (ed) Strategies to Modify the Drug Release from Pharmaceutical Systems. Woodhead Publishing, Sawston, UK; pp 63–86. https://doi.org/10.1016/B978-0-08-100092-2.00005-9
23. EFSA Panel on Plant Health (2015) Scientific opinion on the pest categorisation of *Spodoptera littoralis*. EFSA J 13:3987. https://doi.org/10.2903/j.efsa.2015.3987
24. Moustafa MAM, Osman EA, Mokbel E-SMS et al. (2024) Biochemical and molecular characterization of chlorantraniliprole resistance in Spodoptera littoralis (*Lepidoptera: Noctuidae*). Crop Prot 177:106533. https://doi.org/10.1016/j.cropro.2023.106533
25. Campolo O, Giunti G, Russo A et al. (2018) Essential oils in stored product insect pest control. J Food Qual 2018:6906105. https://doi.org/10.1155/2018/6906105
26. Sciortino M, Scurria A, Lino C et al. (2021) Silica-microencapsulated orange oil for sustainable pest control. Adv Sust Syst 5:2000280. https://doi.org/10.1002/adsu.202000280
27. Santos A, Santos C, Belino N, et al. (2018) Encapsulation of essential oils in silica coating. In: Proceedings of the 6th International Virtual Conference on Advanced Scientific Results. pp 168–172. https://www.researchgate.net/publication/327821290_Encapsulation_of_Essential_Oils_in_Silica_Coating
28. Lopes RP, Parreira LA, Venancio AN et al. (2023) Chemical characterization and evaluation of acaricidal potential of rosemary essential oil and its main compound α-pinene on the two-spotted spider mite, *Tetranychus urticae*. Nat Prod Res 37:2940–2944. https://doi.org/10.1080/14786419.2022.2137799
29. Aqeel U, Parwez R, Aftab T et al. (2023) Silicon dioxide nanoparticles suppress copper toxicity in *Mentha arvensis* L. by adjusting ROS homeostasis and antioxidant defense system and improving essential oil production. Environ Res 236: 116851. https://doi.org/10.1016/j.envres.2023.116851
30. Indiamart, Rosemary Oil. Price: INR 1,500/kg, July 2025. https://www.indiamart.com/proddetail/rosemary-oil-3026224473.html. Accessed 16 Jul 2025
31. He QJ, Zhang ZW, Gao Y et al. (2009) Intracellular localization and cytotoxicity of spherical mesoporous silica nano- and microparticles. Small 5:2722. https://doi.org/10.1002/smll.200900923
32. Robertson JL, Jones MM, Olguin E, et al. (2017) Bioassays with arthropods. In: 3rd (ed) CRC Press. Boca Raton, FL, USA.
33. Lee MJ, Lee SE, Kang MS et al. (2018) Acaricidal and insecticidal properties of *Coriandrum sativum* oils and their major constituents extracted by three different methods against stored product pests. Appl Biol Chem 61:481–488. https://doi.org/10.1007/s13765-018-0379-z